

A hybrid (ablation-expansion) model for low-density foams

L. Hudec¹, A. Gintrand², J. Limpouch¹, R. Liska¹, S. Shekhanov²,
V. Tikhonchuk^{2,3}, and S. Weber²

¹ FNSPE, Czech Technical University in Prague, Czech Republic

² ELI-Beamlines Center, Institute of Physics of the ASCR, Dolni Brezany, Czech Republic

³ CELIA, University of Bordeaux, CNRS, CEA, Talence, France

36th European Conference on Laser Interaction with Matter

19.9.2022 **ECLIM2022***



eli



Hydrodynamic simulations of laser-foam interaction:

Homogeneous simulation overestimates laser propagation - Foam microstructure have to be included

Direct simulations [Kapin et al (2006), Milovich et al (2021)] - **computationally expensive, limited foam types**

Two-scale models = conventional macroscale hydrodynamics + simplified microscale interaction model

- CTU+CELIA [Velechovský et al (2016)]: expansion of 1D layer, **closed-pore foams only**

- ENEA [Cipriani et al (2018), Gus'kov et al (2015)]: viscosity-dampened decompression, **overcritical foams**

- LLNL [Belyaev et al (2020)]: self-similar isothermal expansion, **small-pore light foams $\rho_{av} < 5 \text{ mg/cm}^3$**

Our area of interest: wire-like chemical aerogel foams/ artificial ("3D printed") foams $\sim 10 \text{ mg/cm}^3$

size of solid elements \gg laser skin depth \rightarrow **surface absorption and ablation**

size of solid elements comparable to laser wavelength \rightarrow wave-based description

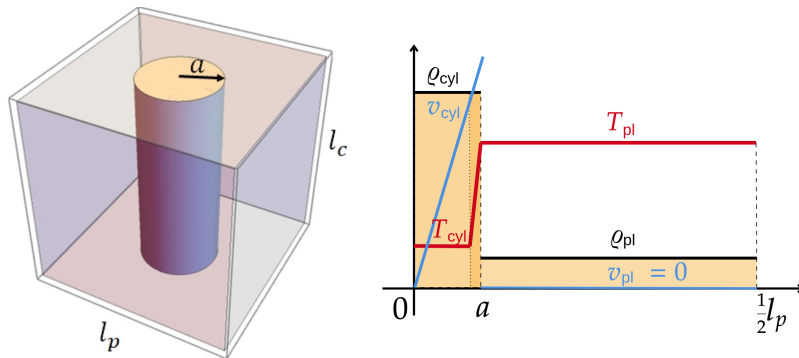
Interaction of laser with sub-wavelength sized cylinder - PIC/hydro simulations by S. Shekhanov and A. Gintrand

as a basis for **Ablation-expansion microscale model**



Microscale model

Conservation laws (PDEs) \rightarrow integration over volume of the pore \rightarrow ODEs for averaged values
6 equations for cylinder radius $a(t)$ and mass $m_{\text{cyl}}(t)$, expansion velocity $v_{\text{exp}}(t)$, and internal energies ε_{cyl} , ε_{pe} , ε_{pi}



Expansion of the cylinder (controlled by cylinder temperature)

Ablation of the cylinder (external flux controlled) - removes mass from the cylinder surface

Pore homogenisation finished when density of cylinder and plasma equilibrate (at average foam density)

Energy conversion process - 3 steps: laser absorption by electrons \rightarrow kinetic energy of accelerated mass \rightarrow ion-ion collisions in plasma \rightarrow ion internal energy (\approx instantaneous in our model, uniform redistribution of mass inside pore)

The total absorption rate per unit length

$$K_{\text{tot}} = K_{\text{cyl}} + K_{\text{pl}}$$

Absorption in the plasma

$$K_{\text{pl}} = K_{\text{ib}}(\varrho_{\text{pl}}, T_{\text{pe}}) \left(1 - \frac{\pi a^2 l_c}{V_{\text{pore}}}\right)$$

Inverse bremsstrahlung weighted by volume

Absorption in the cylinder

overcritical cylinder $\varrho_{\text{cyl}} > \varrho_{\text{cr}}$

$$K_{\text{cyl}} = Q_{\text{abs}} \frac{2al_c}{V_{\text{pore}}}$$

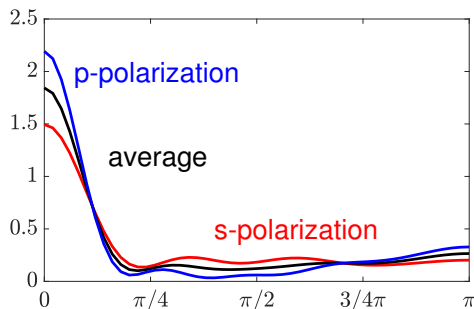
effective cross-section

subcritical cylinder $\varrho_{\text{cyl}} < \varrho_{\text{cr}}$

$$K_{\text{cyl}} = K_{\text{ib}}(\varrho_{\text{cyl}}, T_{\text{cyl}}) \frac{\pi a^2 l_c}{V_{\text{pore}}}$$

weighted inverse bremsstrahlung

Efficiency factors $Q_{\text{abs}} \simeq 0.5 - 1.0$, $Q_{\text{sca}} \simeq 1 - 3$ from Mie theory of electromagnetic scattering on cylindrical particles [H. C. van der Hulst, *Light scattering by small particles* (Dover Publ., 1957)]



Laser scattering on cylindrical foam elements:
Angular distribution

$$p_{\text{sca}}(\theta) = \frac{s(\theta) P_{\text{sca}}}{l_p l_c I_{\text{las}}} \approx s(\theta) \left[1 - \exp\left(-Q_{\text{sca}} \frac{2a}{l_p}\right)\right]$$

Cumulative distribution function \approx two-step profile



Macroscale ray-tracing use K_{tot} to calculate the total power deposited to pore P_{las}

Absorbed power in cylinder

$$P_{\text{cyl}} = \eta_{\text{cyl}} P_{\text{las}}$$

Absorbed power in plasma

$$P_{\text{ib}} = \eta_{\text{ib}} P_{\text{las}}$$

$$\eta_{\text{cyl}} = \frac{K_{\text{cyl}}}{K_{\text{tot}}}, \quad \eta_{\text{ib}} = \frac{K_{\text{pl}}}{K_{\text{tot}}}, \quad \eta_{\text{cyl}} + \eta_{\text{ib}} = 1$$

The energy flux entering the surface of the cylinder

$$q_{\text{cyl}} = \frac{P_{\text{cyl}}}{2\pi a l_c} + q_{\text{th}}$$

Local electron heat conduction between plasma and cylinder

$$q_{\text{th}} = f_{\text{lim}} \frac{Z_{\text{max}} \rho_{\text{pl}}}{m_i} k_B v_{te} (T_{pe} - T_{\text{cyl}})$$

(calculated as a fraction of a free-streaming limit)

Heating of cylinder

$$q_{\text{heat}} = \zeta_{\text{las}} \frac{P_{\text{cyl}}}{2\pi a l_c} + \zeta_{\text{th}} q_{\text{th}}$$

Ablation

$$q_{\text{abl}} = \underbrace{(1 - \zeta_{\text{las}}) \frac{P_{\text{cyl}}}{2\pi a l_c}}_{q_{\text{abl,las}}} + \underbrace{(1 - \zeta_{\text{th}}) q_{\text{th}}}_{q_{\text{abl,th}}}$$

Parameters ζ_{las} , ζ_{th} control the splitting of the fluxes \rightarrow determines the regime of operation



Expansion and ablation

Radius of the cylinder - combined effect of expansion and ablation:

$$\frac{da}{dt} = v_{\text{exp}} - v_{\text{abl}}$$

Self-similar expansion [Belyaev et al (2018)]

$$\frac{dv_{\text{exp}}}{dt} = \frac{4}{3} \frac{\varepsilon_{\text{cyl}}}{a} \Theta(T_{\text{cyl}} - T_{\text{exp}})$$

- expansion suppressed for low temperatures
(foam not sufficiently ionised)

Stationary ablation model [Manheimer et al (1982)]

- two contributions: laser and local heat flux

$$v_{\text{abl,las}} = \frac{(2q_{\text{abl,las}}\rho_{\text{cr}}^2)^{1/3}}{2\rho_{\text{cyl}}} \quad \left| \quad v_{\text{abl,th}} = \frac{3q_{\text{abl,th}}}{2\rho_{\text{cyl}}(\varepsilon_{\text{pe}} + \varepsilon_{\text{pi}})} \right. \quad \text{Thermal ablation [Betti et al (2001)]}$$

$$v_{\text{abl}} = \xi_a v_{\text{abl,las}} \Theta(\rho_{\text{cyl}} - \rho_{\text{cr}}) + v_{\text{abl,th}}$$

- laser ablation turned off in subcritical cylinder
- average over laser polarisations, additional factor $\xi_a \approx 0.5$

Mass of the cylinder:

$$\frac{dm_{\text{cyl}}}{dt} = - \frac{2\pi a l_c v_{\text{abl}} \rho_{\text{cyl}}}{\text{mass ablation rate}} = - \frac{2v_{\text{abl}}}{a} m_{\text{cyl}}, \quad m_{\text{pl}} = m_0 - m_{\text{cyl}}$$



Energy balance

Specific internal energy of cylinder:

$$\frac{d\varepsilon_{\text{cyl}}}{dt} = -\frac{1}{2a} v_{\text{abl}} v_{\text{exp}}^2 - \frac{2}{3} \frac{v_{\text{exp}}}{a} \varepsilon_{\text{cyl}} \Theta(T_{\text{cyl}} - T_{\text{exp}}) + \frac{2\pi a l_c}{m_{\text{cyl}}} q_{\text{heat}}$$

kinetic energy of cylinder expansion
cylinder heating

Electron/ion internal energy of plasma inside the pore:

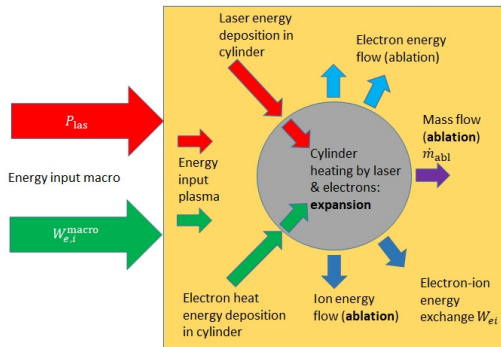
$$\frac{d\varepsilon_{\text{pe}}}{dt} = -\frac{2v_{\text{abl}}}{a} \frac{m_{\text{cyl}}}{m_{\text{pl}}} \varepsilon_{\text{pe}} + \frac{2v_{\text{abl}}}{a} \frac{m_{\text{cyl}}}{m_{\text{pl}}} (1 - \zeta_i) \left(\varepsilon_{\text{cyl}} + \frac{1}{2} v_{\text{exp}}^2 \right) + (1 - \zeta_i) \frac{2\pi a l_c}{m_{\text{pl}}} q_{\text{abl}} - \frac{2\pi a l_c}{m_{\text{pl}}} q_{\text{th}} + \frac{P_{\text{ib}}}{m_{\text{pl}}} - W_{\text{ei}} + W_e^{\text{macro}}$$

energy from the ablation flux
local HF
electron heatflux from neighbouring pores

$$\frac{d\varepsilon_{\text{pi}}}{dt} = -\frac{2v_{\text{abl}}}{a} \frac{m_{\text{cyl}}}{m_{\text{pl}}} \varepsilon_{\text{pi}} + \frac{2v_{\text{abl}}}{a} \frac{m_{\text{cyl}}}{m_{\text{pl}}} \zeta_i \left(\varepsilon_{\text{cyl}} + \frac{1}{2} v_{\text{exp}}^2 \right) + \zeta_i \frac{2\pi a l_c}{m_{\text{pl}}} q_{\text{abl}} + W_{\text{ei}} + W_i^{\text{macro}}$$

energy from the ablation flux
ion heatflux from neighbouring pores

Mass and energy balance in a pore



Free parameter ζ_i controls the repartition of energy between electrons/ions ($\zeta_i \approx 0.6$ in PIC simulations)



Microscale-macroscopic connection

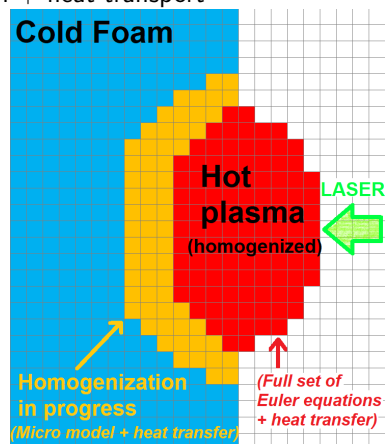
Macroscale - two-temperature Euler equations with the electron/ion heat conductivity, electron-ion energy exchange, and laser source term (in fully homogenised cells)

In non-homogenised cells: microscale model + laser absorption + heat transport

Modifications to the macroscale hydrodynamics:

- Laser deposition is calculated using a modified absorption rates/coefficients
- Hydrodynamic motion is suppressed in non-homogenised cells
- ODEs for the microscale model solved (with a reduced timestep) using RK4 method
- Internal energy and the kinetic energy of the expanding cylinder "hidden" from macroscale, added at the end of homogenisation:

$$\Delta \varepsilon_e = \frac{m_{\text{cyl}}}{m_0} \frac{Z_{\text{cyl}}}{Z_{\text{cyl}} + 1} \varepsilon_{\text{cyl}}, \quad \Delta \varepsilon_i = \frac{m_{\text{cyl}}}{m_0} \left(\frac{1}{Z_{\text{cyl}} + 1} \varepsilon_{\text{cyl}} + \frac{1}{4} v_{\text{exp}}^2 \right)$$



Hybrid model implemented in **PALE** (Lagrangian/ALE code) and **FLASH** (Eulerian code)

Simulation in one foam pore

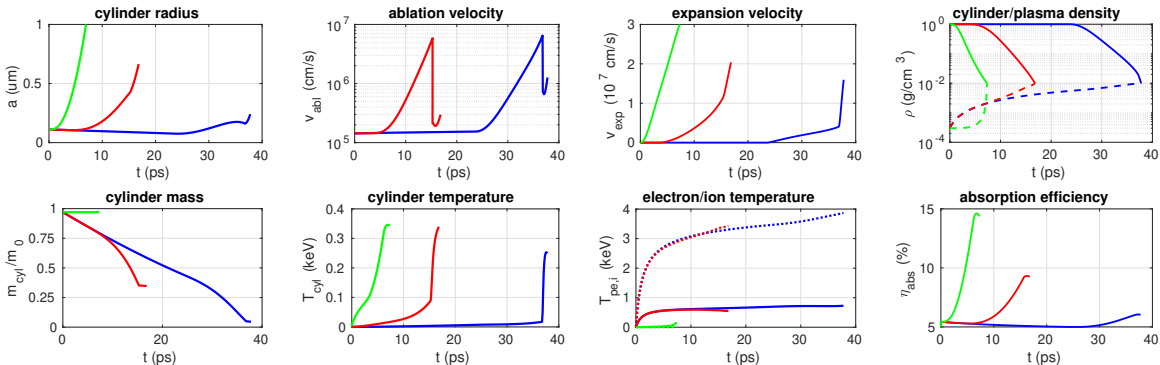
One-pore test for the laser intensity 10^{14} W/cm²; no interaction with neighbouring cells/pores
Foam target similar to [V. Tikhonchuk et al, (2021)]

The free parameters of the model determine the regime of operation:

Expansion dominated regime ($\zeta_{\text{las}} = 1$) - fast, 7 ps homogenisation time

Combined regime ($\zeta_{\text{las}} = 0, \zeta_{\text{th}} = 0.5$) - intermediate, 16 ps

Ablation dominated regime ($\zeta_{\text{las}} = 0, \zeta_{\text{th}} = 10^{-2}$) - slow, 38 ps

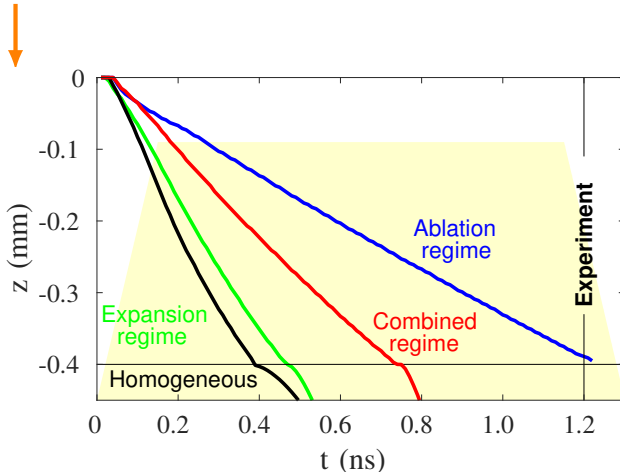


Other parameters: $Q_{\text{abs}} = 0.5, \xi_{\text{abl}} = 0.5, \zeta_i = 0.5, T_{\text{exp}} = 5$ eV, $f_{\text{lim}} = 0.03$

Comparison of hybrid model results to the experimental data

Ionisation wave front propagation

LASER



Experiment at the Shenguang III prototype laser [V. Tikhonchuk et al (2021)]

0.4 mm thick target

10 mg/cc TMPTA foam, 2 μ m pores

Laser energy 835 J / 1.3 ns pulse

Peak laser intensity $2 \cdot 10^{14}$ W/cm²

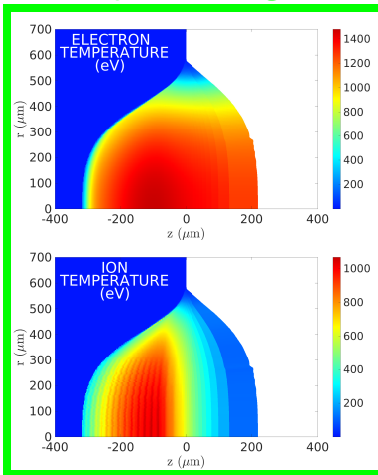
4th order super-gaussian spatial profile

Target burned-through at 1.2 ns

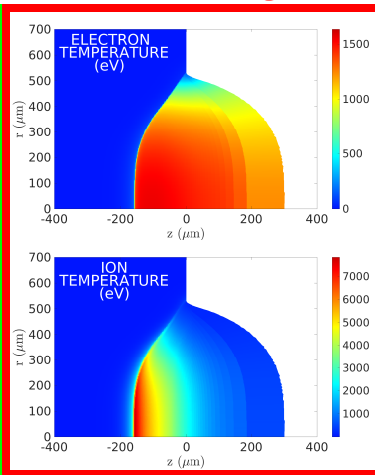
Results from PALE code, front edge of target at $z = 0$ mm
(scattering on foam microstructure enabled)



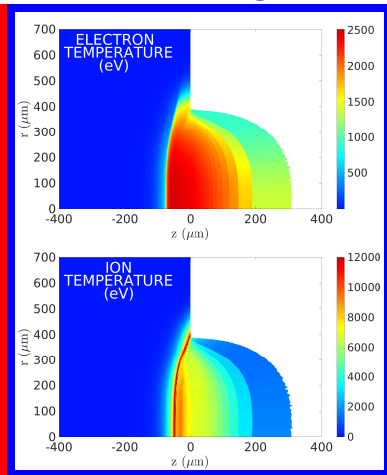
Expansion regime



Combined regime



Ablation regime



Temperature profiles at 300 ps

ion temperature $T_i \approx 4T_e \approx ZT_e$

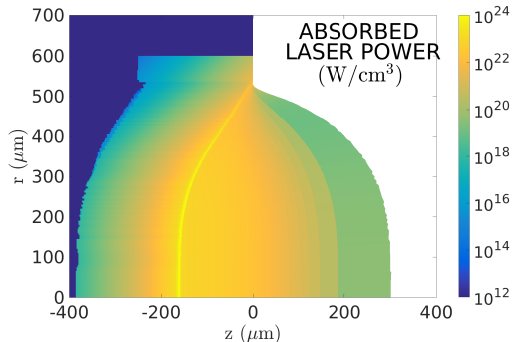


The influence of random foam scattering

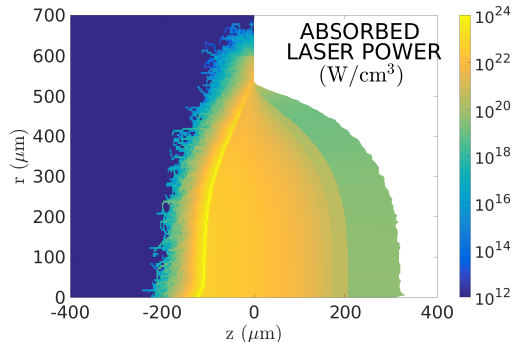
Random scattering decreases laser penetration through foam layers

Smaller width of the homogenisation region \rightarrow decreases propagation speed by 20-25 %

Without scattering



With scattering



Deposited laser power at 300 ps



- We presented a novel approach to the foam modelling that combines a self-similar expansion of cylindrical elements with a surface ablation by laser
- Three regimes of operation have been demonstrated in one-pore test of the model
- The hybrid model has been applied to simulate the experiment at the Shenguang III prototype laser
- The inclusion of foam-induced laser scattering is crucial for the foam simulations as it reduces the laser penetration and decreases the width of the homogenisation zone

Thank you for your attention

